An Apparent General Solution for the Kinetic Models of the Bacteriorhodopsin Photocycles

Richard W. Hendler

Laboratory of Cell Biology, National Heart, Lung, and Blood Institute, National Institutes of Health, Bethesda, Maryland 20892

Received: May 24, 2005; In Final Form: June 15, 2005

For the past decade, the field of Bacteriorhodopsin (BR) research has been influenced by a kinetic view of the photocycle as a reversible, homogeneous, model (RHM) with a linear sequence of intermediates. More recently, we proposed a much different model which consists of essentially unidirectional, parallel (i.e., heterogeneous) cycles (UPM) (Hendler, R. W.; Shrager, R. I.; Bose, S. *J. Phys. Chem. B* **2001**, *105*, 3319−3328). It is important to try to resolve which of the two models is more likely to be correct, because models influence and provide a basis for further experimentation. Therefore, in this communication, we reexamine the basis for the RHM with a focus on the most recent and complete description of this model (van Stokkum, I., H., M.; Lozier, R. *J. Phys. Chem. B* **2002**, *106*, 3477−3485) vis a vis the UPM in an in-depth study. We show that (i) the tested RHM does not really work for the data of van Stokkum and Lozier nor ours; (ii) no previously published RHM model has been shown to work for data under any conditions; (iii) there are many published observations that are difficult if not impossible to explain by RHM, but are readily explained by parallel cycles. It is also shown that either a UPM or a parallel cycle model with limited reversibility correctly describes photocycle data collected at pH 5, 7, and 9 and at 10, 20, and 30° and is consistent with all known experimental observations.

Introduction

For at least 25 years[1] it has been known that the intensity of the exciting light markedly alters the ratio of two different kinetic forms of M intermediate in the wild-type Bacteriorhodopsin (BR) photocycle. It was realized that either a photocooperative effect of light on a homogeneous population of BR or the existence of a heterogeneous population of BR molecules is required to explain this important observation. Shrager et al.[2] showed that mathematical models based on either principle could be constructed that were compatible with the experimental observations so that some more direct means were needed to resolve the question of photocooperativity and homogeneity vs heterogeneity as the cause for the observation. The photocooperativity explanation is that a single photon hit on the BR-trimer initiates a photocycle containing a single M (i.e., M1), whereas a multiple photon impact initiates a different photocycle in which the M intermediate is of the M_2 type. The heterogeneity explanation involves two separate populations of BR. The one that produces M1 is present in a lesser amount but presents a larger target size for photon capture. Therefore, at low light flux it is predominant, but at higher light levels, the cycle containing M_2 becomes predominant.

Hendler et al.[3,4] showed that a specifically defined kinetic model consisting of two unidirectional parallel cycles (UPM) could account for kinetic experimental data obtained after laser flash activation of the BR photocycle under ambient conditions at pH 7. This model, applied to the experimental data, deconvoluted the overlapping experimental kinetic spectra by retrieving absolute spectra for the photocycle intermediates. In a later paper,[5] Shrager and Hendler reviewed publications based on reversible homogeneous photocycles (RHM) and concluded that, as of 2003, no RHM had been demonstrated to be capable of denconvoluting raw experimental data into the isolated absolute intermediate spectra based on the fitted kinetic macroconstants appropriate for the collected data.

Recently, a complete RHM has been published.[6] This RHM is unique in several respects. It provides all of the kinetic microconstants necessary for testing the model; the authors were able to extract absolute intermediate spectra from experimental data by applying the model, and, by mutual agreement between the two groups, it has been possible to share data and methods used in both experimental approaches to compare directly the UPM and RHM model data sets collected at pH 7 and 20 °C. Thanks to the gift of Lozier of data collected at pH 5, 7, and 9 and at temperatures of 10, 20 and 30 °C, it has also been possible to see if a UPM solution is appropriate for data collected under a variety of conditions.

The fact that both the UPM of Hendler et al. and the RHM of van Stokkum and Lozier were able to retrieve acceptable absolute spectra from raw data collected at pH 7 and 20 °C presents a problem. At best, only one or the other can be true for the BR photocycle. The goal of the present investigation is to resolve this problem and to present a thorough and in-depth discussion on the merits of either a RHM or UPM paradigm for the BR photocycle. It is concluded that the UPM provides a better solution for data collected at pH 7 and 20 °C. Using the criterion of obtaining clean isolated spectra for all intermediates from raw data, the UPM was also satisfactory for data collected at pH 5 and 30 °C and at pH 9 and both 10 and 20 °C. For data collected at pH 7 at both 10 and 30° and at pH 9 and 30 °C, a partially reversible parallel model (PRPM) was required to extract clean spectra from the data.

Methods

Data. The data set used by van Stokkum and Lozier[6] for the RHM consists of 15 wavelengths from 300 to 700 nm, separated by steps of 20 nm and 47 log-spaced time points from 0.001 to

10.1021/jp052733h
Published on Web 08/06/2005

300 ms. These data were generated by Xie et al.[7] and kindly provided to us by Richard Lozier. Data acquired under parallel polarization conditions were used, to be compatible with most published kinetic studies on the BR photocycle.

Mathematical Procedures. The mathematical procedures employed have been described in detail elsewhere[3,4] and only a brief description to guide the reader is provided here. For more complete information, the cited publications should be consulted.

A. The UPM[3] at pH 7 and 20°.

$$(1)\ BR_1^* \xrightarrow{k1} K_1 \xrightarrow{k2} L_1 \xrightarrow{k3} M_1 \xrightarrow{k6} N \xrightarrow{k5} O \xrightarrow{k7} BR$$

$$(2)\ BR_2^* \xrightarrow{k1} K_2 \xrightarrow{k3} L_2 \xrightarrow{k4} M_2 \xrightarrow{k7} BR$$

The fitted kinetic macro decay constants are:

tau (ms)	k (ms^{-1}) (fastest to slowest)
(1) 3.4812e-004	2.8726e+003
(2) 1.4107e-003	7.0887e+002
(3) 3.7364e-002	2.7664e+001
(4) 1.2189e-001	8.2041e+000
(5) 5.1346e-001	1.9476e+000
(6) 2.8427e+000	3.5178e-001
(7) 7.2975e+000	1.3703e-001

This model is completely specified by a system of ordinary differential equations, expressed in matrix form by $dy/dt = Jy$, where y = the amounts of each state in the photocycle and

$$J = \begin{array}{c} \begin{matrix} BR_1^* & K_1 & L_1 & M_1 & N & O & BR_2 & K_2 & L2 & M_2 \end{matrix} \\ \begin{bmatrix} -k1 & 0 & 0 & 0 & 0 & 0 & 0 & 0 & 0 & 0 \\ k1 & -k2 & 0 & 0 & 0 & 0 & 0 & 0 & 0 & 0 \\ 0 & k2 & -k3 & 0 & 0 & 0 & 0 & 0 & 0 & 0 \\ 0 & 0 & k3 & -k6 & 0 & 0 & 0 & 0 & 0 & 0 \\ 0 & 0 & 0 & k6 & -k5 & 0 & 0 & 0 & 0 & 0 \\ 0 & 0 & 0 & 0 & k5 & -k7 & 0 & 0 & 0 & 0 \\ 0 & 0 & 0 & 0 & 0 & 0 & -k1 & 0 & 0 & 0 \\ 0 & 0 & 0 & 0 & 0 & 0 & k1 & -k2 & 0 & 0 \\ 0 & 0 & 0 & 0 & 0 & 0 & 0 & k2 & -k4 & 0 \\ 0 & 0 & 0 & 0 & 0 & 0 & 0 & 0 & k4 & -k7 \end{bmatrix} \end{array}$$

The initial conditions are

$$y0 = [\ f1 \quad 0 \quad 0 \quad 0 \quad 0 \quad 0 \quad f2 \quad 0 \quad 0 \quad 0\ ]$$

where $f1$ and $f2$ are fitted parameters for the fractions of first and second cycles present. Because the J-matrix for the unidirectional system is lower triangular, the diagonal contains eigenvalues, the reciprocals of which are equal to the fitted macro time constants obtained from the raw data.

As described previously,[3,4] the time courses for the growth and decay of each intermediate in the photocycle in a matrix Y can be found using Matlab as follows:

```
% ----- Eigensystem & mixing matrix ---------------------------------
 [ W, K ] = eig(J);                  % Eigensystem of J.
 K = diag(K);
 M = W*diag(W\y0);                   % Mixing matrix.
 Y = M*exp(K*t');                    % Time courses for Y obtained by mixing eigenvalues of J
 Y = [ Y;   1 - sum(Y) ];            % Supplement Y to obtain absolute spectra
% -------Obtain absolute spectra from Y ------------------------------
```

The quality of spectra obtained depends on the parameter $y0$, which, in this case, contains $f1$ and $f2$, the starting amounts of each component that undergoes turnover and contributes to the intermediate spectra. The bulk of BR ($1 - (f1 + f2)$) does not turnover and is present as a constant background. To retrieve authentic spectra for the photocycle intermediates, best values for $f1$ and $f2$ are obtained by an iterative least squares regression process. The spectra that we seek to obtain should be for each intermediate alone and therefore free of other processes such as light scattering and end absorption. We find that a cubic polynomial constructed with four coefficients using absorbances at wavelengths 400, 440, 680, and 700 nm of the ground-state spectrum leads to a background curve that matches absorbances at both ends of the BR spectrum and provides smooth curve for the non-BR background. Minimal spectral criteria are used in the fitting process to obtain $f1$ and $f2$; namely, (i) the absorbance for species BR, L, and N should be minimal below 425 nm; (ii) the absorbance for M should be minimal above 500 nm; (iii) the absorbance for O should be minimal below 550 nm. Beyond these weak constraints, no specific shape is imposed for the absolute spectra of the intermediate species. A criterion for acceptance of a tested model is that the wavelengths of maximum absorbance for all components be very close to those determined for the isolated intermediates, as reported in the literature from many laboratories using a variety of procedures independent from any kinetic model (Table 1).

Most of the determinations in Table 1 proceed by obtaining difference spectra at a series of increasing delay times after a laser flash. Different pHs or temperatures or mutants to enhance the accumulation of particular intermediates have been used. The fraction of BR that has turned over is estimated, and appropriate scaling factors are employed to determine the amount of BR ground spectra to be added to the difference spectra to obtain absolute spectra of the accumulated intermediates at particular points in time. In some cases, other procedures are employed; for example, Becher et al.[9] used cryogenic techniques to trap intermediates. Gergely et al.[12] used SVD to obtain a basis set of difference spectra, U. A low noise data set, D, was reconstituted from U and S and V. Then, a model-independent Monte Carlo method with constraints was used to find time courses from which accurate difference spectra could be obtained from the filtered data in D. Absolute spectra were obtained by adding scaled amounts of BR to the difference spectra. Borucki et al.[13] used transient linear dichroism in combination with transient absorbance data to help define unique solutions for separation of intermediates. Kulcsar et al.[14] used SVD with self-modeling to determine individual absolute spectra.

It is generally agreed that M_1 and M_2 have either identical spectra or spectra that are too close to resolve. Similar considerations apply to a species that appears in more than one parallel cycle. Therefore, instead of trying to resolve separate spectra for a given species (such as M or L) that appears more than once in a photocycle, the time courses for these intermediates in matrix Y are combined to a new matrix of time courses, Y_s. Then the set of absolute spectra (D_s) are obtained by

$$D_s = A/Y_s$$

where $/Y_s$ is the pseudoinverse of Y_s.

B. The RHM[6] at pH 7 and 20°.

$$K \rightleftarrows L \rightleftarrows M_1 \rightleftarrows M_2 \rightleftarrows N \rightleftarrows O \rightarrow BR$$

TABLE 1: Characteristic Wavelengths (nm) of Maximum Absorbance for BR Photocycle Intermediates

	1 (ref 8)	2 (ref 9)	3 (ref 10)	4 (ref 11)	5 (ref 12)	6 (ref 13)	7 (ref 14)	8 (this work)	9 (this work)
BR	570	568	570	572	570	573	568	569	570
K	590	628			586	599	588		590
L	550	547	550		544	541	542	550	550
M	412	412	412	409	409		410	412	412
N				568	562		552	569	584
O	640		640	635	629		630	636	640

At pH 7 and 20 °C, the published values of the kinetic microconstants (s^{-1}) are:

$k1$	$K \rightarrow L$	428000 ± 2000
$k2$	$K \leftarrow L$	110000 ± 1000
$k3$	$L \rightarrow M_1$	11400 ± 700
$k4$	$L \leftarrow M_1$	6700 ± 1000
$k5$	$M_1 \rightarrow M_2$	3800 ± 1200
$k6$	$M_1 \leftarrow M_2$	2600 ± 500
$k7$	$M_2 \leftarrow N$	490 ± 70
$k8$	$M_2 \leftarrow N$	120 ± 20
$k9$	$N \rightarrow O$	500 ± 70
$k10$	$N \leftarrow O$	470 ± 100
$k11$	$O \rightarrow BR$	700 ± 120

This model is completely specified by a system of ordinary differential equations, expressed in matrix form by $dy/dt = Jy$, where $y =$ the amounts of each state in the photocycle and

$$J = \begin{array}{c} \begin{matrix} K & L & M_1 & M_2 & N & O \end{matrix} \\ \begin{bmatrix} -k1 & k2 & 0 & 0 & 0 & 0 \\ k1 & -(k2+k3) & k4 & 0 & 0 & 0 \\ 0 & k3 & (k4+k5) & 0 & 0 & 0 \\ 0 & 0 & k5 & -(k6+k7) & k8 & 0 \\ 0 & 0 & 0 & k7 & -(k8+k9) & 0 \\ 0 & 0 & 0 & 0 & k9 & -(k10+k11) \end{bmatrix} \end{array}$$

The initial conditions are

$$y0 = [1 \;\; 0 \;\; 0 \;\; 0 \;\; 0 \;\; 0]$$

The same procedures described above for the UPM are used to obtain first the time courses in Y_s and then the absolute spectra in D_s from the raw data matrix A.

Source of the J-Matrix. As shown above, the J-matrix expressed in the form of a set of ordinary differential equations specifically describes a kinetic model. If both the structure of J and the values of all of the kinetic constants are known, then the validity of J as a true model for a set of experimental kinetic data can be tested. The tested model is considered validated if two conditions are met. (1) The spectra for all intermediates should show absorbance maxima at wavelengths in accordance with those agreed upon by many different laboratories. Each isolated spectrum should be present, essentially free of any appreciable contamination by spectra of other intermediates. (2) The macro kinetic constants specified by the eigenvalues of the J-matrix should be the same as the macro kinetic constants obtained in a least squares regression analysis of the data using a sums-of-exponentials model.

In the case of RHM, one assumes that a particular representation may be valid and the values of all micro constants are determined by experimental procedures. This is true for the RHM tested here.

In the case of UPM, an entirely different approach is used to define the J-matrix. All possible unidirectional models that can be constructed from the fitted exponentials are tested. As previously explained, this includes single linear sequences, sequences with branches, and parallel cycles.[3,4] By fitting exponentials to the raw data in matrix A, one can obtain the model-independent difference spectra in a matrix C that are associated with each fitted exponential macro constant in a matrix X so that $A = CX$. For example, in a case where 6 exponentials are required to fit a set of data, there will be a single difference spectrum for each exponential in X. There are 6! or 720 permutations of linking order for these exponentials, all of which are tested as described below. Sequences for all permutations involving only 5 and 4 of the exponentials are also tested. When all of the fitted exponentials are tested, the orders of both the exponentials in X and corresponding spectra in C are rearranged to correspond to each tested permutation. When linear sequences with fewer exponentials are tested, only the same number of corresponding spectra in C are used. It is obvious for cases where six or more exponentials are involved, a very large number of linear sequences must be evaluated. Fortunately, we have been able to develop computer-based algorithms which can quickly and efficiently search through all of the permutations to find only viable sequences.[3,4] By viable, it is meant that (i) the spectral properties of difference spectra should clearly involve the known photocycle states of BR, K, L, M, N, and O; (ii) the order of the intermediates should be consistent with the order just listed; (iii) the initial and final states should be BR; (iv) any transition must involve the decay of only a single component coupled with the rise of a single component; (v) when an intermediate is formed in a transition step, it must be the species that decays in the subsequent transition step; (vi) the earliest transitions should clearly be BR $\rightarrow$ K $\rightarrow$ L $\rightarrow$; and (vii) the amplitudes for the intermediates should be consistent with the amount of ground-state BR.

As a result of applying filters which reject sequences that do not meet all conditions, one ends with a small number of linear sequences of various lengths that are consistent with the data set. J-matrices are then constructed from all combinations of the surviving linear sequences to see if acceptable absolute spectra can be obtained for all of the intermediates and that the eigenvalues specified by the J-matrix are the same as the kinetic macro constants obtained by fitting the data to a sums-of-exponentials model.[3,4] If any nonacceptable absolute intermediate spectrum is found or if the eigenvalues and fitted constants do not agree, then the tested model is rejected. If no UPM is possible, none will be found. If a parallel cycles model is valid but reversibility exists in certain of the transitions, one would expect to find an absolute spectrum showing both species of the reversible couple present. This is, in fact what has occurred under certain of the tested conditions.

Testing for Limited Reversibility in a Photocycle where Two Adjacent Intermediate Spectra Are Seen in an Isolated Spectrum for a Single Intermediate. The eigenvalues of the J-matrix are equal to the macro kinetic decay constants of the

system specified by the matrix. For a J-matrix that is lower diagonal, the eigenvalues are the diagonal elements of the matrix. All unidirectional kinetic models are represented by lower diagonal matrices. Reverse rate constants always appear in the upper diagonal space so that the relationship between diagonal elements and eigenvalues no longer holds. Therefore, when testing whether a reverse rate can be introduced, there must be a way to compensate the new rate constant by adjustment of the microconstants leading to and from the intermediate that will be affected so that all of the eigenvalues of the new J-matrix will remain equal to the experimentally determined macro kinetic decay constants. The procedures described here were designed to allow a reverse constant to be introduced without changing eigenvalues and to allow an iterative process to adjust forward and reverse microconstants while determining the turnover rates and deducing absolute intermediate spectra.

Consider a unidirectional reaction sequence linking two intermediates, and let the rate constant $k_{i,j}$ pertain to the transition to y_i from y_j:

$$y1 \xrightarrow{k21} y2 \xrightarrow{k32}$$

This sequence is represented by the matrix equation

$$dy/dt = Jy$$

where J is lower bidiagonal.

$$J = \begin{bmatrix} -r1 & 0 \\ r1 & -r2 \end{bmatrix}$$

where $r1 = k21$ and $r2 = k32$ The macroscopic rate constants, denoted as r_1 and r_2, can be found by inspection, because they are exhibited on the main diagonal of J. That is, the macroscopic rate constants, which are also the eigenvalues of J, are found on the main diagonal of J *provided J is of lower triangular form*. In our work, these constants have been found by fitting sums of exponentials to kinetic data. Once found, the macroscopic rate constants are held fixed while the model is fitted to idealized species spectra using fractions cycling and optional reverse rate constants as parameters. The problem is that a reverse rate constant appears above the main diagonal of J, thus deviating from the lower triangular form of J in the unidirectional model. How does one introduce such a quantity into J without altering the eigenvalues of J?

Without belaboring the algebra, if a reverse constant is isolated, i.e., without a reverse rate in either the previous step or following step of the reaction, the problem can be solved by considering only the two species involved in the reverse reaction, i.e., y_1 and y_2. Isolation does not mean that there can be only one reverse rate in a cycle. For example, in a cycle with six intermediates, there can be as many as three reverse rates, as long as they are not in consecutive steps. So far, our results have needed at most one reverse step per cycle even though the method allows for more.

The subscript 3 refers to the transition to some third species (or simply a sink) which is not otherwise involved in the reaction. The J matrix for the reverse version is

$$J = \begin{bmatrix} -k_{2,1} & k_{1,2} \\ k_{2,1} & -(k_{3,2} + k_{1,2}) \end{bmatrix}$$

Note that the subscripts 1, 2, and 3 can be any trio of successive indexes within the cycle. Note also that if the species 2 is not the final species in the cycle, then the element $k32$ will appear in the third row of J and must be altered there as well. Given r_1, r_2, and the desired reverse constant $k_{1,2}$, our goal is to find $k_{2,1}$ and $k_{3,2}$ such that the eigenvalues of the two versions of J are the same. The characteristic equation of the second form of J is

$$(x - k_{2,1})(x - k_{3,2} - k_{1,2}) - k_{2,1}k_{1,2} = 0$$

and one need only find $k_{2,1}$ and $k_{3,2}$ so that the two solutions of the above quadratic equation in x will be the desired r_1 and r_2. In essence, we are adjusting the forward rate constants to compensate for the reverse rate constant.

Since the solution involves more algebra than we wish to present here, we will simply state the solution with pertinent restrictions. To start, all values of r and k must be real and positive. The reverse rate must be isolated as described above. The reverse rate constant must lie in the range

$$0 < k_{1,2} < (\sqrt{r1} - \sqrt{r2})^2$$

The values r_1 and r_2 are unequal, because all eigenvalues in a given cycle must be distinct for the exponential solution to pertain. Let $b = r_1 + r_2 - k_{1,2}$, and $d = b^2 - 4r_1r_2$. There are two cases:

$$\text{For } r_1 > r_2\text{: } k_{2,1} = 0.5(b + \sqrt{d}) \text{ and } k_{3,2} = r_1 r_2/k_{2,1}$$

$$\text{For } r_1 < r_2\text{: } k_{3,2} = 0.5(b + \sqrt{d}) \text{ and } k_{2,1} = r_1 r_2 / k_{3,2}$$

In an algorithm based on these equations, given the unidirectional constants $r1$ and $r2$ and the tested reverse constant $k12$, the altered forward constants k21 and k32 which will not change the eigenvalue when the reverse constant applies, are returned. When no altered forward constants are compatible with the tested reverse constant; values of -1 are returned.

In the procedures used to obtain absolute spectra for UPM, three minimal spectral constraints are used to find the amounts of turnover for each single cycle in the UPM. For a three-cycle UPM, three turnover parameters (p) are fitted. In testing whether there is an acceptable reverse constant that will lead to clean absolute spectra and unchanged eigenvalues, the microscopic reverse kinetic constant is added to the parameter list for least squares regression analysis. If more than a single reverse constant is to be tested, an additional parameter for each new constant is added to the parameter list.

Results

For detailed statistical fitting data, see Supporting Information.

1. Fitting the RHM Model[6] to Data of Xie et al.[7] at pH 7 and 20 °C. Figure 1 shows that using our procedures described in Methods, with the data of van Stokkum and Lozier[6] and their published constants and turnover fraction (0.19), we can reproduce their spectra. The L-spectrum shows a small range of negative values and the M-spectra show long stretches with significant negative absorbances. These spectra closely resemble the spectra in Figure 5 of van Stokkum and Lozier[6] in the common wavelengths of both data sets.

Figure 2 shows that by fitting the turnover fraction, the negative absorbances were removed from the M and L spectra, but the quality of the O spectrum was decreased.

2. Fitting the RHM Model to Data of Hendler et al.[3] at pH 7 and 20°. Figure 3 shows intermediate spectra obtained applying the RHM to the data of Hendler et al. using the published constants 19% turnover fraction of van Stokkum and

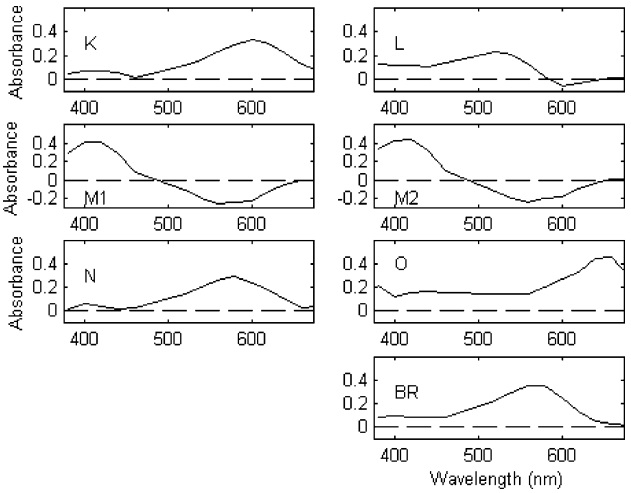

Figure 1. Intermediate spectra obtained using the RHM and published[6] *k* values and 19% turnover fraction.

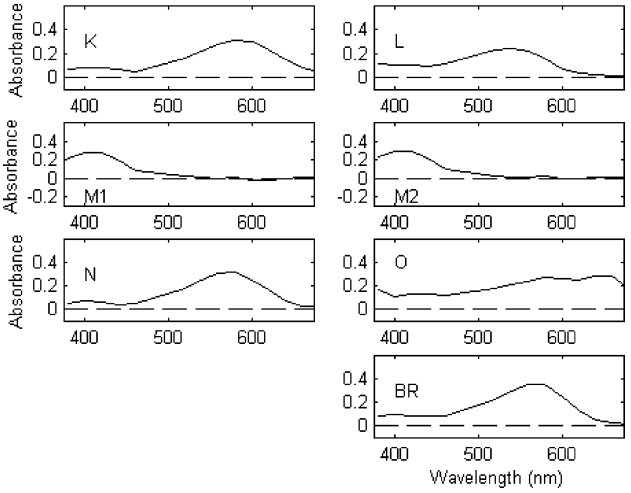

Figure 2. Intermediate spectra obtained using the RHM and published[6] *k* values with fitting turnover based on our minimal constraints.

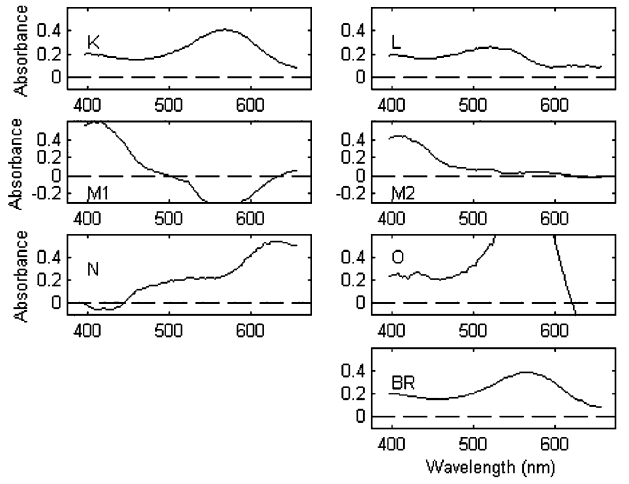

Figure 3. Intermediate spectra obtained using the RHM[6] and the data of Hendler et al.,[3] and the published eigenvalue taus and 19% turnover for BR.[6]

Lozier. The spectra obtained for the M1, N, and O intermediates are unacceptable.

Figure 4 shows intermediate spectra obtained applying the RHM[6] to the data of Hendler et al.[3] using a new set of micro

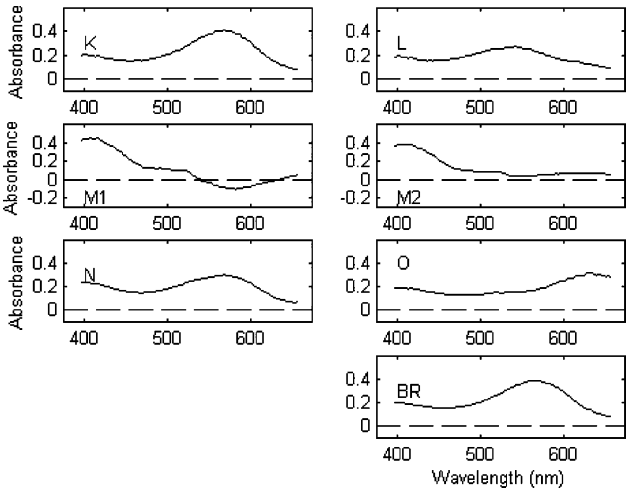

Figure 4. Intermediate spectra obtained using the RHM,[6] the data of Hendler et al.,[3] a new set of *k* values generated by Ivo van Stokkum that are more suitable for these data, and the fitting of turnover.

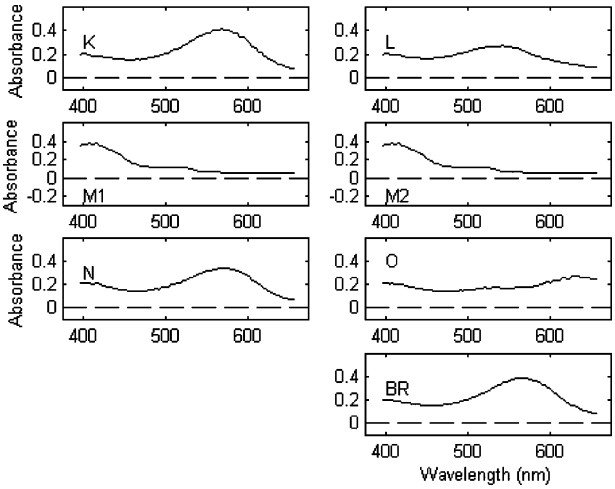

Figure 5. Same as the legend for Figure 4, except that the spectra for M_1 and M_2 were combined.

constants provided by van Stokkum. The fraction of turnover was determined by fitting to be 27%. The overall quality of the spectra is markedly improved compared to Figure 3. The microconstants, however, are markedly different from those obtained by the Eyring-based procedures used by van Stokkum et al. on their data.[6]

Figure 5 shows intermediate spectra obtained applying the RHM[6] to the data of Hendler et al.[3] using the a new set of constants provided by van Stokkum. In this case, the time courses for M_1 and M_2 were combined prior to deriving the turnover fraction and isolated spectra. The fitted turnover was 32%. The overall quality of the spectra is markedly improved compared to Figures 3 and 4 and to the spectra published by van Stokkum and Lozier[6]. The microconstants, however, are markedly different from those obtained by van Stokkum and Lozier for data acquired under very similar conditions of pH and temperature and deduced by Eyring-based procedures applied to data taken over a temperature range. The eigenvalues of the J-matrix are not equal to the fitted macroconstants for the data set used.

3. Fitting the UPM Model to Data of Xie et al.[7] under Different Conditions of pH and Temperature. The designation BR* is used to denote photon-activated ground state.

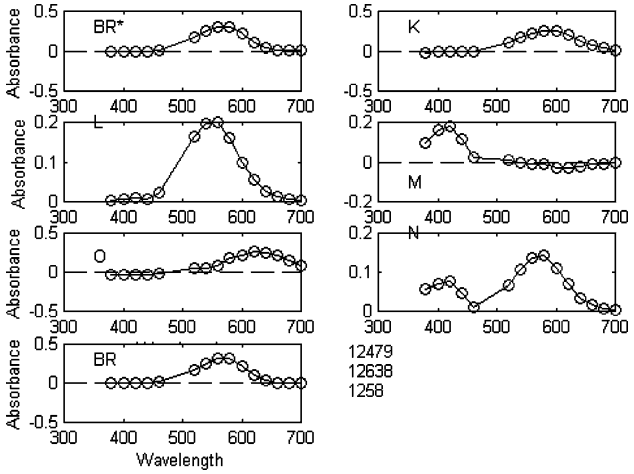

Figure 6. Fit of UPM to data of Xie et al.[7] at pH 7 and 10 °C. Experimental points are shown as small circles. Numbers at lower right signify the order of taus for each cycle.

a. pH 7 and 10 °C. Nine exponentials and three parallel cycles account for the collected raw data.

tau (ms)	k (ms^{-1})
(1) 5.2632e-004	1.9000e+003
(2) 2.9571e-003	3.3817e+002
(3) 9.5657e-003	1.0454e+002
(4) 8.5565e-002	1.1687e+001
(5) 2.3029e-001	4.3424e+000
(6) 7.1175e-001	1.4050e+000
(7) 7.3080e+000	1.3684e-001
(8) 2.3489e+001	4.2573e-002
(9) 7.9317e+001	1.2608e-002

The fitted tau and k values are

$$(1)\ \mathrm{BR^*} \xrightarrow{1} \mathrm{K} \xrightarrow{2} \mathrm{L_1} \xrightarrow{4} \mathrm{M_1} \xrightarrow{7} \mathrm{O} \xrightarrow{9} \mathrm{BR}$$

$$(2)\ \mathrm{BR^*} \xrightarrow{1} \mathrm{K} \xrightarrow{2} \mathrm{L_2} \xrightarrow{6} \mathrm{M_2} \xrightarrow{3} \mathrm{N} \xrightarrow{8} \mathrm{BR}$$

$$(3)\ \mathrm{BR^*} \xrightarrow{1} \mathrm{K} \xrightarrow{2} \mathrm{L_3} \xrightarrow{5} \mathrm{M_3} \xrightarrow{8} \mathrm{BR}$$

The numbers above the arrows designate which taus are used according to their order from fastest to slowest.

Derived absolute spectra in Figure 6 were obtained for a total turnover of 38% with relative turnovers of 7% for cycle (1), 35% for cycle (2), and 58% for cycle (3).

Figure 6 shows the absolute spectra obtained using the model and constants described above. The peak absorbances for all spectra occur at acceptable wavelengths, but the N spectrum shows significant contamination by M, which is indicative of reversibility between the two species under the tested condition. Figure 7 shows that this is indeed the cause of the M contamination of the N spectrum.

The introduction of a reverse N → M_2 step in cycle 2 was found to produce an absolute spectrum free of M contamination (Figure 7). The relative amounts of turnover for each cycle in this case were 9, 29, and 58% of the total. The standard errors and dependencies for fitting turnovers were low. The reverse rate N → M_2 (61.0337 ms^{-1}) was 140% of the forward rate M_2 → N (43.4464 ms^{-1}). The eigenvalues of the new J matrix agreed with the fitted kinetic macroconstants to at least five decimal places.

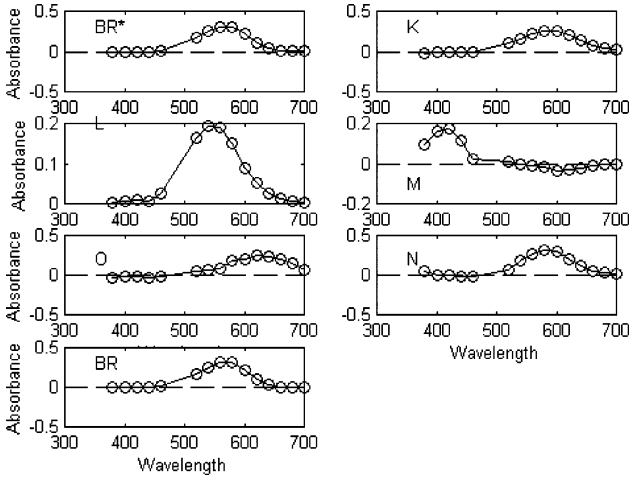

Figure 7. Absolute spectra for intermediates in the three-cycle UPM found for the data at pH 7 and 10 °C with a reversible step between M_2 and N in cycle 2. Experimental points are shown as small circles.

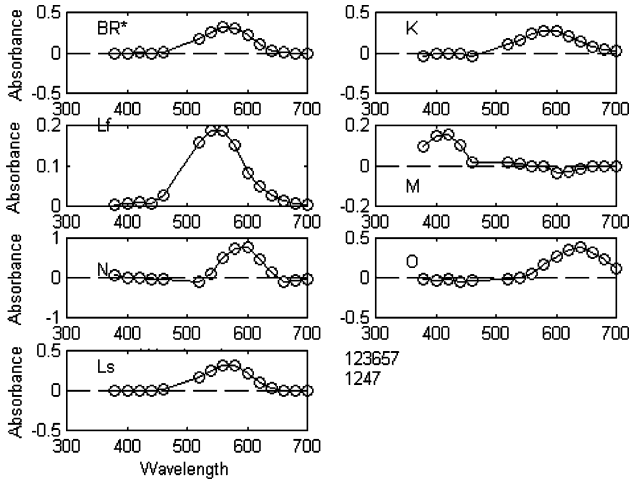

Figure 8. Fit of UPM to data of Xie et al.[7] at pH 7 and 20 °C. Experimental points are shown as small circles. Numbers at lower right signify the order of taus for each cycle.

b. pH 7 and 20 °C. Seven exponentials and two parallel cycles account for the raw data.

tau (ms)	k (ms^{-1})
(1) 3.4812e-004	2.8726e+003
(2) 1.4107e-003	7.0887e+002
(3) 3.7364e-002	2.7664e+001
(4) 1.2189e-001	8.2041e+000
(5) 5.1346e-001	1.9476e+000
(6) 2.8427e+000	3.5178e-001
(7) 7.2975e+000	1.3703e-001

$$(1)\ \mathrm{BR^*} \xrightarrow{1} \mathrm{K} \xrightarrow{2} \mathrm{L_1} \xrightarrow{3} \mathrm{M_1} \xrightarrow{6} \mathrm{N} \xrightarrow{5} \mathrm{O} \xrightarrow{7} \mathrm{BR}$$

$$(2)\ \mathrm{BR^*} \xrightarrow{1} \mathrm{K} \xrightarrow{2} \mathrm{L_2} \xrightarrow{4} \mathrm{M_2} \xrightarrow{7} \mathrm{BR}$$

The numbers above the arrows designate which taus are used.

Derived absolute spectra in Figure 8 were obtained for total turnover of 31% with relative turnovers of 17% for cycle (1) and 83% for cycle (2). The N spectrum was free of contamination by M.

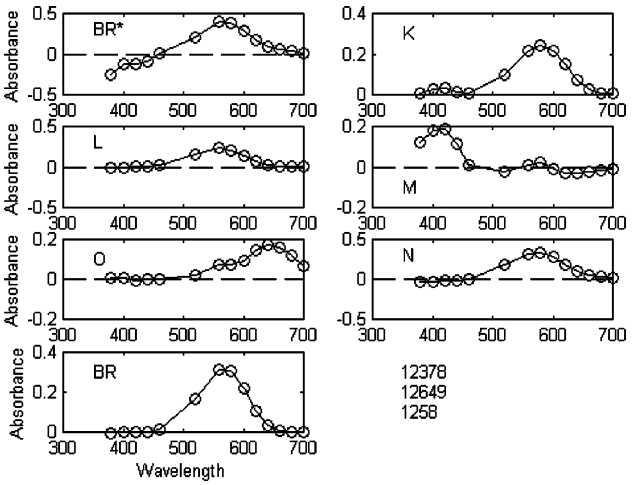

Figure 9. Fit of UPM to data of Xie et al.[7] at pH 7 and 30°. Experimental points are shown as small circles. Numbers at lower right signify the order of taus for each cycle.

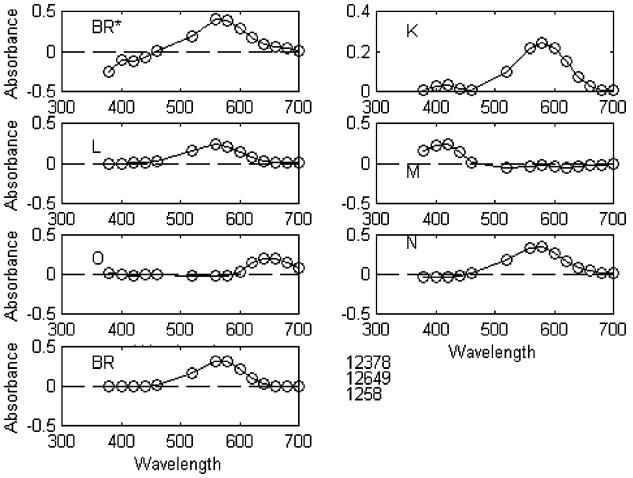

Figure 10. Absolute spectra for intermediates in the 3-cycle UPM found for the data at pH 7 and 30 °C with a reversible step between M_2 and N in cycle 2. Experimental points are shown as small circles.

c. pH 7 and 30 °C. Nine exponentials and three parallel cycles account for the data.

tau (ms)	k (ms^{-1})
(1) 4.5000e-004	2.2222e+003
(2) 7.6175e-004	1.3128e+003
(3) 1.0081e-002	9.9197e+001
(4) 6.7554e-002	1.4803e+001
(5) 2.0948e-001	4.7737e+000
(6) 3.7072e+000	2.6975e-001
(7) 6.8902e+000	1.4513e-001
(8) 1.7797e+001	5.6189e-002
(9) 3.9401e+001	2.5380e-002

$$(1)\ \mathrm{BR^*} \xrightarrow{1} \mathrm{K} \xrightarrow{2} \mathrm{L_1} \xrightarrow{3} \mathrm{M_1} \xrightarrow{7} \mathrm{O} \xrightarrow{8} \mathrm{BR}$$

$$(2)\ \mathrm{BR^*} \xrightarrow{1} \mathrm{K} \xrightarrow{2} \mathrm{L_2} \xrightarrow{6} \mathrm{M_2} \xrightarrow{4} \mathrm{N} \xrightarrow{9} \mathrm{BR}$$

$$(3)\ \mathrm{BR^*} \xrightarrow{1} \mathrm{K} \xrightarrow{2} \mathrm{L_3} \xrightarrow{5} \mathrm{M_3} \xrightarrow{8} \mathrm{BR}$$

The numbers above the arrows designate which taus are used.

Derived absolute spectra in Figure 9 were obtained for a total turnover of 40% with relative turnovers of 24% for cycle (1), 36% for cycle (2), and 40% for cycle (3). In the spectrum for M, there appears to be some N present near 580 nm and there is a shoulder in the spectrum for O. Figure 10 shows that the introduction of an $N \rightarrow M_2$ back reaction improved both of these intermediate spectra.

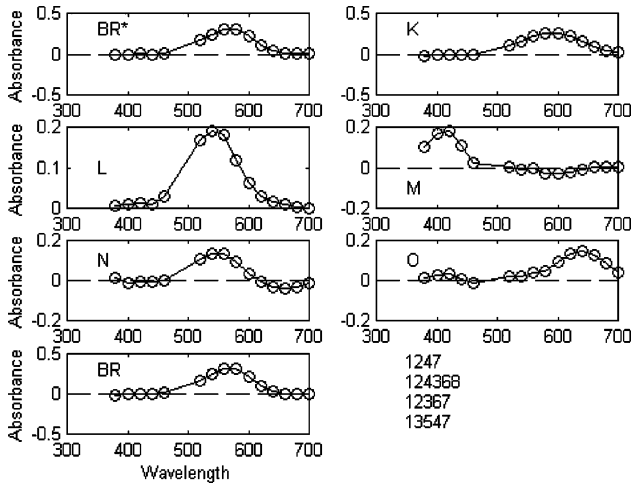

Figure 11. Absolute spectra for intermediates in the four-cycle UPM found for data at pH 5 and 10 °C. The numbers in the lower right-hand corner show the sequence of taus for each cycle listed below.

The introduction of a reverse $N \rightarrow M_2$ step in cycle 2 was found to remove the contaminating presence of N in the isolated spectra for M and O shown in Figure 9. The relative amounts of turnover for each cycle in this case were 19, 49, and 33% of the total compared to 24, 36, and 40% for the UPM shown in Figure 9. The standard errors and dependencies for fitting turnovers were low. The reverse rate $N \rightarrow M_2$ (0.67 ms^{-1}) was 4.7% of the forward rate $M_2 \rightarrow N$ (14.13 ms^{-1}). The eigenvalues of the new J-matrix agreed with the fitted kinetic macroconstants to at least five decimal places.

d. pH 5 and 10 °C. Nine exponentials and four parallel cycles account for the data.

tau (ms)	std. errors	dependencies
(1) 3.9411e-004	8.7674e-006	1.1775e+000
(2) 2.9908e-003	2.1962e-005	1.2369e+000
(3) 1.0608e-001	6.9132e-003	2.0852e+000
(4) 2.8455e-001	9.7927e-003	2.0833e+000
(5) 2.0878e+000	4.6652e-001	1.5061e+000
(6) 9.6019e+000	6.1992e-001	1.5530e+000
(7) 3.3744e+001	1.0800e+000	2.7492e+000
(8) 1.4260e+002	1.1384e+002	2.6123e+000

Sum squares: 4.3212e−005

$$(1)\ \mathrm{BR^*} \xrightarrow{1} \mathrm{K} \xrightarrow{2} \mathrm{L} \xrightarrow{4} \mathrm{M} \xrightarrow{7} \mathrm{BR}$$

$$(2)\ \mathrm{BR^*} \xrightarrow{1} \mathrm{K} \xrightarrow{2} \mathrm{L} \xrightarrow{4} \mathrm{M} \xrightarrow{3} \mathrm{N} \xrightarrow{6} \mathrm{O} \xrightarrow{8} \mathrm{BR}$$

$$(3)\ \mathrm{BR^*} \xrightarrow{1} \mathrm{K} \xrightarrow{2} \mathrm{L} \xrightarrow{3} \mathrm{M} \xrightarrow{6} \mathrm{O} \xrightarrow{7} \mathrm{BR}$$

$$(4)\ \mathrm{BR^*} \xrightarrow{1} \mathrm{K} \xrightarrow{3} \mathrm{L} \xrightarrow{5} \mathrm{M} \xrightarrow{4} \mathrm{N} \xrightarrow{7} \mathrm{BR}$$

The numbers above the arrows designate which taus are used.

Derived absolute spectra in Figure 11 were obtained for a total turnover fraction of 36% with relative turnovers of 66% for cycle (1), 11% for cycle (2), 15% for cycle (3), and 8% for cycle 4.

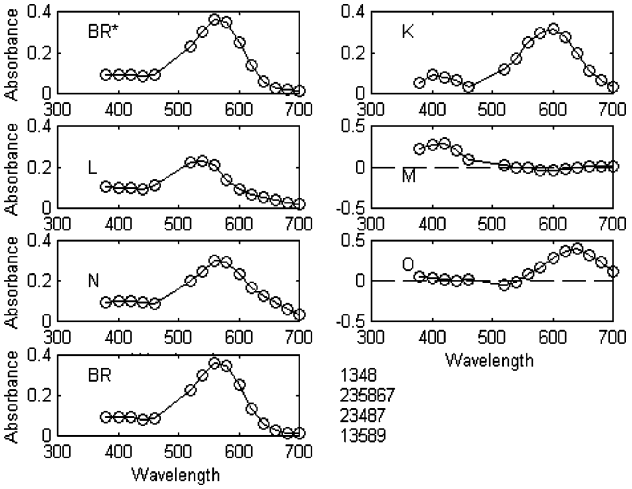

Figure 12. Absolute spectra for intermediates in the four-cycle UPM found for data at pH 5 and 20 °C.

e. pH 5 and 20 °C. Nine exponentials and four parallel cycles account for the data.

tau (ms)	std. errors	dependencies
(1) 5.0000e-005	2.1344e+001	3.9259e+000
(2) 2.8818e-004	1.0417e-004	4.1189e+000
(3) 1.4973e-003	1.9465e-005	1.3361e+000
(4) 4.9553e-002	1.7167e-003	2.2548e+000
(5) 1.3606e-001	3.2522e-003	2.2620e+000
(6) 1.8065e+000	2.0242e-001	2.7373e+000
(7) 3.9105e+000	2.3661e-001	2.8731e+000
(8) 1.1286e+001	2.6426e-001	2.4479e+000
(9) 3.3716e+001	5.5970e+000	2.2283e+000

Sum squares: 1.1777e−005

$$(1)\ \mathrm{BR}^* \xrightarrow{1} \mathrm{K} \xrightarrow{3} \mathrm{L} \xrightarrow{4} \mathrm{M} \xrightarrow{8} \mathrm{BR}$$

$$(2)\ \mathrm{BR}^* \xrightarrow{2} \mathrm{K} \xrightarrow{3} \mathrm{L} \xrightarrow{5} \mathrm{M} \xrightarrow{8} \mathrm{N} \xrightarrow{6} \mathrm{O} \xrightarrow{7} \mathrm{BR}$$

$$(3)\ \mathrm{BR}^* \xrightarrow{2} \mathrm{K} \xrightarrow{3} \mathrm{L} \xrightarrow{4} \mathrm{M} \xrightarrow{8} \mathrm{O} \xrightarrow{7} \mathrm{BR}$$

$$(4)\ \mathrm{BR}^* \xrightarrow{1} \mathrm{K} \xrightarrow{3} \mathrm{L} \xrightarrow{5} \mathrm{M} \xrightarrow{8} \mathrm{N} \xrightarrow{9} \mathrm{BR}$$

Derived absolute spectra in Figure 12 were obtained for a total turnover fraction of 21% with relative turnovers of 1% for cycle (1), 12% for cycle (2), 58% for cycle (3), and 30% for cycle (4).

f. pH 5 and 30 °C. Eight exponentials and four parallel cycles account for the data.

tau (ms)	std. errors	dependencies
(1) 4.3819e-004	6.0858e-005	1.5138e+000
(2) 7.5301e-004	3.8247e-005	1.6967e+000
(3) 9.8099e-003	1.3404e-003	2.2285e+000
(4) 8.4498e-002	4.9440e-003	2.7321e+000
(5) 3.2604e-002	1.6116e-003	3.6155e+000
(6) 7.2563e-001	3.4429e-002	1.9587e+000
(7) 2.3578e+000	3.5050e-002	2.0054e+000
(8) 5.5284e+000	2.7169e-002	1.3069e+000

Sum squares: 8.9163e-006

$$(1)\ \mathrm{BR}^* \xrightarrow{1} \mathrm{K} \xrightarrow{2} \mathrm{L} \xrightarrow{4} \mathrm{M} \xrightarrow{8} \mathrm{BR}$$

$$(2)\ \mathrm{BR}^* \xrightarrow{1} \mathrm{K} \xrightarrow{2} \mathrm{L} \xrightarrow{5} \mathrm{M} \xrightarrow{7} \mathrm{N} \xrightarrow{6} \mathrm{O} \xrightarrow{8} \mathrm{BR}$$

$$(3)\ \mathrm{BR}^* \xrightarrow{1} \mathrm{K} \xrightarrow{2} \mathrm{L} \xrightarrow{3} \mathrm{M} \xrightarrow{7} \mathrm{O} \xrightarrow{8} \mathrm{BR}$$

$$(4)\ \mathrm{BR}^* \xrightarrow{1} \mathrm{K} \xrightarrow{2} \mathrm{L} \xrightarrow{4} \mathrm{M} \xrightarrow{5} \mathrm{N} \xrightarrow{8} \mathrm{BR}$$

The numbers above the arrows designate which taus are used.

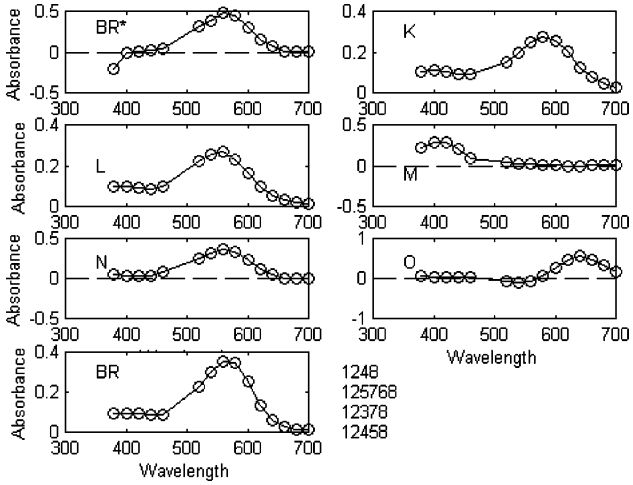

Figure 13. Absolute spectra for intermediates in the four-cycle UPM found for the data at pH 5 and 30 °C.

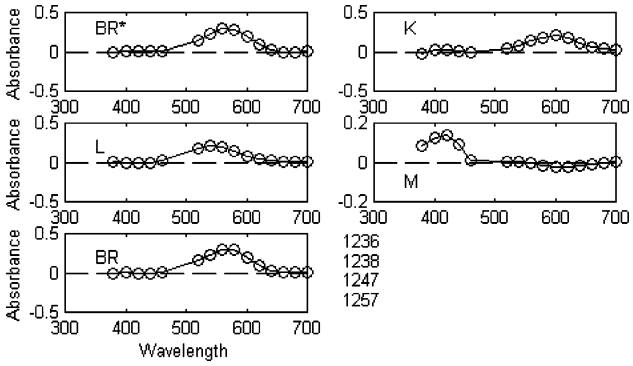

Figure 14. Absolute spectra for intermediates in the four-cycle UPM found for the data at pH 9 and 10 °C.

Derived absolute spectra in Figure 13 were obtained for a total turnover fraction of 40% with relative turnovers of 54% for cycle (1), 5% for cycle (2), 14% for cycle (3), and 27% for cycle (4).

g. pH 9 and 10 °C. Eight exponentials and four parallel cycles account for the data.

tau (ms)	std. errors	dependencies
(1) 5.5131e-004	2.5274e-005	1.2844e+000
(2) 2.8074e-003	7.8846e-005	1.3039e+000
(3) 2.2381e-002	2.9420e-003	1.2282e+000
(4) 1.9686e-001	2.0959e-002	2.1860e+000
(5) 5.7806e-001	7.6147e-002	2.3823e+000
(6) 6.5096e+000	1.0733e+000	2.7000e+000
(7) 2.2906e+001	4.0889e+000	3.5202e+000
(8) 8.6057e+001	9.9997e+000	2.1931e+000

Sum squares: 2.0803e−004

$$\mathrm{BR}^* \xrightarrow{1} \mathrm{K} \xrightarrow{2} \mathrm{L} \xrightarrow{3} \mathrm{M} \xrightarrow{6} \mathrm{BR}$$

$$\mathrm{BR}^* \xrightarrow{1} \mathrm{K} \xrightarrow{2} \mathrm{L} \xrightarrow{3} \mathrm{M} \xrightarrow{8} \mathrm{BR}$$

$$\mathrm{BR}^* \xrightarrow{1} \mathrm{K} \xrightarrow{2} \mathrm{L} \xrightarrow{4} \mathrm{M} \xrightarrow{7} \mathrm{BR}$$

$$\mathrm{BR}^* \xrightarrow{1} \mathrm{K} \xrightarrow{2} \mathrm{L} \xrightarrow{5} \mathrm{M} \xrightarrow{7} \mathrm{BR}$$

The numbers above the arrows designate which taus are used.

Derived absolute spectra in Figure 14 were obtained for a total turnover fraction of 30% with relative turnovers of 14% for cycle (1), 60% for cycle (2), 25% for cycle (3), and 1% for cycle (4).

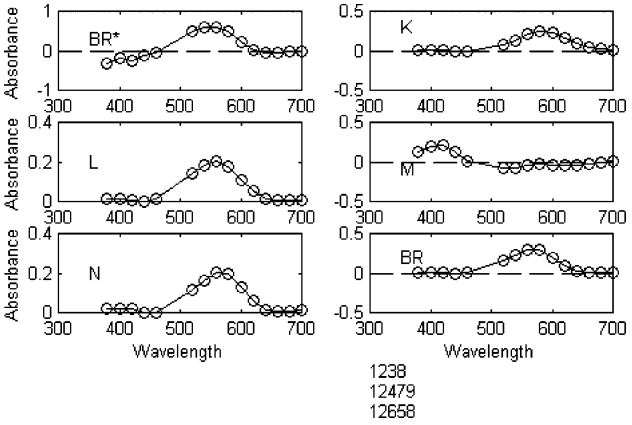

Figure 15. Absolute spectra for intermediates in the three-cycle UPM found for the data at pH 9 and 20 °C.

h. pH 9 and 20 °C. Nine exponentials and three parallel cycles account for the data.

tau (ms)	std. errors	dependencies
(1) 3.0690e-004	3.5176e-005	1.2281e+000
(2) 1.3740e-003	2.1961e-005	1.3332e+000
(3) 1.0586e-002	5.6812e-004	1.6073e+000
(4) 7.8084e-002	2.8064e-003	2.7614e+000
(5) 2.3317e-001	9.3168e-003	2.8711e+000
(6) 1.6005e+000	1.0797e-001	2.6454e+000
(7) 4.3606e+000	2.1455e-001	2.5455e+000
(8) 1.8451e+001	9.7576e-001	2.8570e+000
(9) 4.0812e+001	4.3026e+000	2.2656e+000

Sum squares: 9.2682e−006

$$(1)\ \mathrm{BR^*} \xrightarrow{1} \mathrm{K} \xrightarrow{2} \mathrm{L} \xrightarrow{3} \mathrm{M} \xrightarrow{8} \mathrm{BR}$$

$$(2)\ \mathrm{BR^*} \xrightarrow{1} \mathrm{K} \xrightarrow{2} \mathrm{L} \xrightarrow{4} \mathrm{M} \xrightarrow{7} \mathrm{N} \xrightarrow{9} \mathrm{BR}$$

$$(3)\ \mathrm{BR^*} \xrightarrow{1} \mathrm{K} \xrightarrow{2} \mathrm{L} \xrightarrow{6} \mathrm{M} \xrightarrow{5} \mathrm{N} \xrightarrow{8} \mathrm{BR}$$

The numbers above the arrows designate which taus are used.

Derived absolute spectra in Figure 15 were obtained for a total turnover fraction of 40% with relative turnovers of 11% for cycle (1), 36% for cycle (2), and 53% for cycle (3).

i. pH 9 and 30 °C. Nine exponentials and three parallel cycles account for the data.

tau (ms)	std. errors	dependencies
(1) 4.3392e-005	1.3911e+002	1.4252e+000
(2) 8.6759e-004	2.1335e-005	1.5640e+000
(3) 1.1306e-002	6.7992e-004	1.7570e+000
(4) 5.2197e-002	2.6742e-003	2.2609e+000
(5) 2.0973e-001	5.6918e-002	3.6960e+000
(6) 4.5193e-001	9.3168e-002	3.5676e+000
(7) 1.3445e+000	9.2170e-002	1.6844e+000
(8) 7.0322e+000	5.3175e-001	2.9624e+000
(9) 1.8281e+001	2.2490e+000	2.4920e+000

Sum squares: 3.0650e−005

$$(1)\ \mathrm{BR1^*} \xrightarrow{1} \mathrm{K_1} \xrightarrow{2} \mathrm{L_1} \xrightarrow{6} \mathrm{M_1} \xrightarrow{5} \mathrm{BR}$$

$$(2)\ \mathrm{BR2^*} \xrightarrow{1} \mathrm{K_2} \xrightarrow{2} \mathrm{L_2} \xrightarrow{4} \mathrm{M_2} \xrightarrow{7} \mathrm{N_2} \xrightarrow{8} \mathrm{BR}$$

$$(3)\ \mathrm{BR3^*} \xrightarrow{1} \mathrm{K_3} \xrightarrow{2} \mathrm{L_3} \xrightarrow{3} \mathrm{M_3} \xrightarrow{7} \mathrm{N_3} \xrightarrow{9} \mathrm{BR}$$

Derived absolute spectra in Figure 16 were obtained for a total turnover fraction of 30% with relative turnovers of 17% for cycle (1), 1% for cycle (2), and 82% for cycle (3).

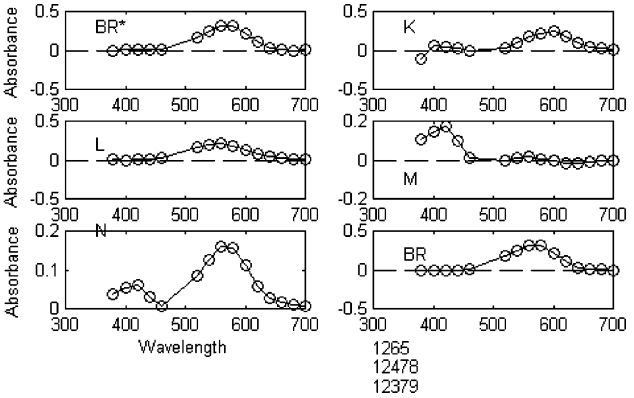

Figure 16. Absolute spectra for intermediates in the three-cycle UPM found for the data at pH 9 and 30 °C.

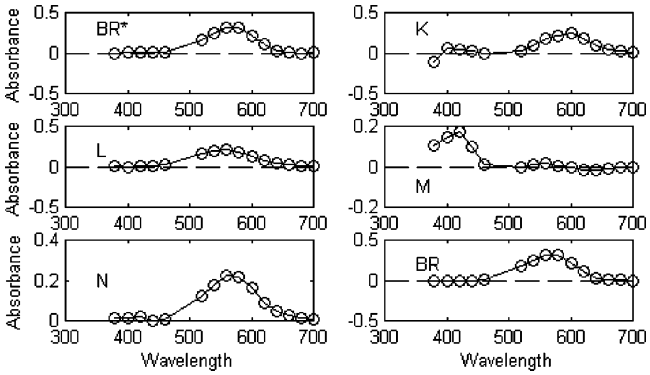

Figure 17. Absolute spectra for intermediates in the three-cycle UPM found for the data at pH 9 and 30 °C with reversible steps between M_2 and N_2 in cycle 2 and between M3 and N3 in cycle 3. Experimental points are shown as small circles.

As was the case for the UPM solution for the data obtained at pH 5 and 10 °C, appreciable contamination of the N spectrum by the M intermediate is seen. The introduction of N → M back reactions in cycles 2 and 3 resulted in an N spectrum free of M contamination (Figure 17).

Reversible steps from N to M in cycles 2 and 3 were introduced and the microconstants to and from the N-intermediates adjusted to maintain the eigenvalues of the J-matrix as described in Methods. The fitted value for the reverse microconstant ($N_2 \rightarrow M_2$) was 0.11777 ms^{-1}, which is 20% of the forward rate of 0.58847 ms^{-1}. The fitted value for the reverse microconstant ($N_3 \rightarrow M_3$) was 0.19753 ms^{-1}, which is 38% of the forward rate of 0.52318 ms^{-1}. The resultant intermediate spectra in Figure 17 shows that the introduction of these reversible steps removed the contaminating M spectrum from the isolated N spectrum.

Discussion

Results Obtained in the Current Studies. The absolute intermediate spectra (AIS) obtained by application of our methods to the data of Xie et al.[7] using the RHM, published kinetic constants, and turnover fraction (0.19) of van Stokkum and Lozier[6] reproduces the spectra they obtained, which show absorption maxima at acceptable wavelength positions, but there are large continuous negative absorption ranges in the M spectra (Figure 1 and ref 6). Furthermore, the eigenvalues of the J matrix describing the RHM are not the same as the macro constants obtained by curve fittings and they differ from values obtained in other laboratories (Table 2). The results shown in Figure 1 are also significant for other reasons. They were obtained in our laboratory, using our methods applied to data of Xie et al.[7]

TABLE 2: Summary of Exponential Time Constants

exponential fittings (taus in ms)[a]				deduced from J matrix[b]
fitters	Hendler[c] and Shrager	Chizhov[d] et al.	Hendler	none
data	Hendler	theirs	Xie and Lozier	Xie and Lozier
tau1	0.005	0.008	0.0014[e]	0.002
tau2	0.05	0.04	0.051	0.056
tau3	0.11	0.12	0.153	0.224
tau4	0.5−1.	0.55	0.882	0.688
tau5	1.7−2.6	1.7	2.6	2.4
tau6	4.5−5.5	5.0	7.0	8.23
tau7	10(20−30)[f]	22		
tau8	70			

[a] For data collected near pH 7 and 20 °C. [b] van Stokkum and Lozier.[6] [c] Ranges and averages from thousands of fittings during many years. [d] Chizhov et al.[59] The $t_{1/2}$ values presented in the publication have been converted to τ's for the table. Very similar values were obtained by Müller et al.[60] using a combination of visible, IR, and photocurrent measurements. [e] A seventh τ of 0.0004 ms was fit to these data. [f] This is the value we obtain, treating taus 7 and 8 as a single component (as did Chizhov et al.).

obtained with polarizers in parallel orientation to each other. The results published by van Stokkum and Lozier[6] were obtained in their laboratory applied to data of Xie et al.[7] obtained with polarizers at the "magic angle". The fact that the AIS obtained here match those published by van Stokkum and Lozier attests to the validity of the procedures used in our laboratory for further evaluation of the data of Xie et al. When we fit the turnover fraction (0.33) using our minimal spectral constraints, the long negative absorption regions for the M intermediates were removed, but the quality of the AIS for the O intermediate was diminished (Figure 2).

The RHM model applied to data of Hendler et al.[3] produced unacceptable AIS (Figure 3), but using a different set of kinetic constants, provided to us by van Stokkum, led to a greatly improved set of AIS from the same data (Figure 4). Combining M_1 and M_2 into a single spectrum produced the best set of AIS from the data (Figure 5). However, the new microconstants for this analysis are markedly different from those determined by van Stokkum and Lozier[6] using an approach based on the Eyring relationship between the logs of the constants and the reciprocals of absolute temperature. Furthermore, the new constants were obtained from only one set of data acquired at a single temperature.

The UPM model applied to data collected at pHs 5, 7, and 9, and temperatures of 10, 20, and 30 °C produced AIS for all intermediates with absorption maxima at expected wavelengths (Figures 6 and 8−16) and with eigenvalues of the J matrix equal to the fitted macroconstants for the raw data. However, in two cases (Figures 6 and 16), there were marked contaminations of the N-spectrum by the M-spectrum. In both instances, it was demonstrated that a modification of the J-matrix for the UPM allowing a back reaction from the N-intermediate to the M-intermediate produced AIS free of contamination (Figures 7 and 17). In Figure 11 (pH 5 and 10 °C) a small peak for M was seen in the isolated spectrum for O. This could be evidence for reversible reactions linking M to O as in M $\rightleftarrows$ N $\rightleftarrows$ O. Similarly, in Figures 10 and 12, a small amount of M is seen in the K spectra, indicating possible reverse reactions in the sequence, K $\rightleftarrows$ L $\rightleftarrows$ M. Our procedure for evaluating back reactions is not applicable for two successive transitions, so we cannot test this possibility. In Figures 9, 13, and 15, the absorbances for some low wavelength absorbancess for the BR* intermediate were negative. Because the decay time constant for BR* is ~0.4 μs, there is extremely limited information for this transition in the collected data, and its closeness in time to the laser flash can be the cause of these outlying data points.

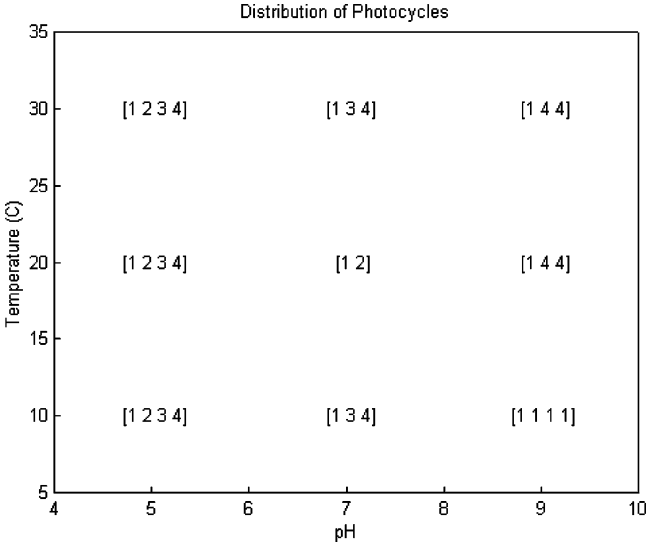

Figure 18. The numbers 1 through 4 represent the four individual photocycles listed in the text that are found to exist under different conditions of pH and temperature.

Influence of pH and Temperature on Cycles in the UPM. In all of the nine different conditions tested, distributions of four basic cycles were found.

$$(1)\ BR^* \rightarrow K \rightarrow L \rightarrow M \rightarrow BR$$

$$(2)\ BR^* \rightarrow K \rightarrow L \rightarrow M \rightarrow N \rightarrow O \rightarrow BR$$

$$(3)\ BR^* \rightarrow K \rightarrow L \rightarrow M \rightarrow O \rightarrow BR$$

$$(4)\ BR^* \rightarrow K \rightarrow L \rightarrow M \rightarrow N \rightarrow BR$$

A plot of these distributions on a grid showing pH and T in two dimensions (Figure 18) has the appearance of a phase diagram. Cycles 2 and 3, which contain the O intermediate, are predominant in the lower pH range. Cycle 2, which contains both the N and O intermediates, is found at all tested temperatures at pH 5 and only at 20 °C at pH 7. At pH 9, only the 4-step cycle-1, and the 5-step cycle-4 are seen. No O-intermediate was detected at pH 9.

Possible Explanation for a Phase-Diagram-like Distribution of Parallel Models. Contemporary research views the lipids of biological membranes as a mosaic of regions of microdomains or "rafts". A collection of some recent papers that speak to these points, as well as instances where lipids markedly affect integral membrane enzyme activity, are cited.[17−23] With this distribution, integral membrane enzymes can be subject to interactions and associations with different lipids depending on their location. In the case of BR, this will lead to a heterogeneity in ground states such as has been reported in the literature (described below). In purple membranes, it has been shown that interactions of BR with specific lipids regulate photocycle pathways, protein conformation, intermembrane mobility of alpha helices, and the kinetics of the photocycle.[24−27] Lipids are subject to melting and phase changes influenced by their composition and changes in condition, such as temperature and pH. Protein−lipid interactions are also influenced by pH and temperature. Such interactions could account for the differences in photocycles under different experimental conditions as found here and in other laboratories (described below).

Minimum Standards for Acceptance of Any Proposed Kinetic Model. We define a kinetic model as a system of ordinary differential equations (ODE) which describes every step involving all intermediates and the precise modes of linkage of these intermediates. The model is expressed mathematically by a Jacobian matrix (J) containing all of the kinetic constants for the ODE. There can be only one correct kinetic model (i.e., J) for the BR photocycle. Any model presumed to represent the photocycle must meet all of the minimum requirements listed below.

Requirement 1. Any proposed model must provide a solution to the equation $A = DY$ where D is a matrix containing all absolute spectra for the intermediates and Y is a matrix containing time courses for each component in D. Usually, some means of estimating either D or Y are used to solve for the other unknown, but as discussed elsewhere, inaccuracy in the provided matrix leads to uncertainty in the deduced matrix.[5] Furthermore, even an accurate solution to this equation, which provides an authentic Y matrix, does not provide the kinetic model that is sought, unless it is possible to derive J from the time courses in Y.

Requirement 2. The J matrix, whether properly derived from an authentic Y or obtained by the procedures described in this paper and elsewhere,[3,4] must contain values for every kinetic micro constant involved.

Requirement 3. The eigenvalues of the J-matrix must be equal to the kinetic macro constants obtained by fitting exponentials to the experimental data.

Requirement 4. Absolute spectra obtained by matrix multiplication A/Y where /Y in the pseudo inverse of Y must be consistent with the spectra deduced from a number of laboratories using both similar and different procedures as described in Table 1.

Requirement 5. The model must be compatible with all established experimental observations pertaining to the BR ground state and its photocycle.

Some Proposed RHM Models. The ten models shown below are made up to accommodate some particular observation that was not compatible with a previous ad hoc model. At the time the model is offered, evidence is presented to demonstrate why it may be true. These models do not attempt to meet any minimum requirements for acceptance as a possibly true model of the BR photocycle based on their application to experimental data. The above list includes two classes of model, A and B. Type A models are incomplete and untestable insofar as numerical values for the proposed kinetic constants are not provided. They are short-lived and often replaced with different RHMs by the same authors who originally proposed them.

(1) $BR \rightleftharpoons K \rightleftharpoons L \rightleftharpoons M_1 \rightleftharpoons M_2 \rightleftharpoons N \rightleftharpoons O \rightleftharpoons BR$ ref 28

(2) $BR \rightleftharpoons J \rightleftharpoons K \rightleftharpoons L \rightleftharpoons M_1 \rightleftharpoons M_2 \rightleftharpoons N \rightleftharpoons O \rightleftharpoons BR$ refs 29, 30

(3) $K \rightleftharpoons L \rightleftharpoons X \rightleftharpoons M \rightleftharpoons N \rightleftharpoons O \rightleftharpoons BR$ ref 31

(4) $L \rightleftharpoons M_1 \rightleftharpoons M_2 \rightleftharpoons N \rightleftharpoons O \rightleftharpoons BR$ at low pH ref 32
$L \rightleftharpoons M_1 \rightleftharpoons M_1' \rightleftharpoons M_2' \rightleftharpoons N' \rightleftharpoons O' \rightleftharpoons BR$ at high pH

(5) $K \rightleftharpoons L \rightleftharpoons M \rightleftharpoons N \rightleftharpoons O \rightleftharpoons BR$ ref 33

(6) $BR \rightleftharpoons J \rightleftharpoons K \rightleftharpoons L \rightleftharpoons M_1 \rightleftharpoons M_2 \rightleftharpoons N \rightleftharpoons O \rightleftharpoons BR$ ref 34

(7) $BR \rightleftharpoons K \rightleftharpoons L \rightleftharpoons M_1 \rightleftharpoons M_2 \rightleftharpoons N \rightleftharpoons O \rightleftharpoons BR$ ref 35

(8) $K \rightleftharpoons L \rightleftharpoons M_1 \rightleftharpoons M_2 \rightleftharpoons N \rightleftharpoons O \rightleftharpoons BR$ ref 36

(9) $K \rightleftharpoons L_1 \rightleftharpoons L_2 \rightleftharpoons M_1 \rightleftharpoons M_2 \rightleftharpoons N_1 \rightleftharpoons N_2 \rightleftharpoons O \rightleftharpoons BR$ ref 37

(10) $BR \rightleftharpoons K \rightleftharpoons L \rightleftharpoons M_1 \rightleftharpoons M_2 \rightleftharpoons M_2' \rightleftharpoons N \rightleftharpoons N' \rightleftharpoons O \rightleftharpoons BR$ ref 38

A. Ad hoc, hypothetical, and incomplete. In example 1, branching at N was included to account for the observation that at low pH, a $N \rightleftharpoons BR$ transformation predominates, whereas at high pH, a $O \rightleftharpoons BR$ transformation predominates. The $L \rightleftharpoons M_1 \rightleftharpoons M_2$ sequence is included because it can account for biphasic kinetics for the M species.

In example 2, the model differs from example 1 by making the transition between K and L reversible. The model was verified by use of the Eyring equation for temperature dependence of the rate constants, using plots of $\ln(k)$ vs $1/T$. More will be said about this approach below and in the Supporting Information.

In example 4, kinetics were studied as a function of pH. A critical factor that influenced the kinetics was whether the ambient pH was greater than or less than the pK of the proton release site X on the extracellular surface. One RHM was seen predominant at low pH and another at high pH.

In example 5, factor analysis and decomposition were used to determine the number of photocycle intermediates from the raw data and then proceed to extract "pure difference spectra" and corresponding time courses that best fit the data. No values for the kinetic microconstants were determined, and minimum requirements for authenticating a solution were not met.

The RHM in example 7 was used as a basis for interpretation of structural changes of intermediates trapped by rapid freezing and analyzed by electron crystallography. Interpretations of structural changes attributed to the isolated intermediates according to this RHM were attributed to a shift in equilibrium between a channel for proton binding being shifted from the extracellular to cytoplasmic surface by light. None of the minimal requirements for proving a model was met.

Example 9 was used as a basis to synthesize data for testing the ability of SVD-SM to extract absolute intermediate spectra. The RHM was based on publications of Varo and Lanyi.[29,30] The model was not applied to analyze experimental data.

In example 10, the model was used as a basis for interpretation of putative X-ray structures of the intermediates BR, K, L, M_1, M_2, and N′ obtained by rapidly cooling photostationary states to trap the intermediates and to prove that during the $M_1 \rightleftharpoons M_2$ step there is a reorientation of a protonation switch from the extracellular to cytoplasmic surface to allow release of a proton to the extracellular surface during the $M_2 \rightleftharpoons M_2'$ step. In the $M_2' \rightleftharpoons N$ step, the Schiff base is reprotonated and in the $N \rightleftharpoons N'$ step, a proton is taken up from the cytoplasmic side. None of the minimal requirements for proving a model was met.

B. Ad hoc, hypothetical, and complete. These models are based on class A models, but evaluations for all of the kinetic constants are provided. These evaluations are derived from experimental data. Examples from the above list include 3, 6, and 8.

Example 3 historically is the first to provide kinetic microconstants for all transitions in the model. The Arrenhius relationship was used in determining all constants at all temperatures. More will be said about this approach below. No restrictions were placed on the spectra for intermediates. The authors recognized that the tested RHM does not properly describe the experimental data.

In example 6, the Eyring equation was used to validate all kinetic constants in the model, as well as to determine the important thermodynamic quantities ΔH (enthalpy), ΔS (entropy), and ΔG (free energy) for all transitions, as well as ΔH^*, ΔS^*, and ΔG^*, the same quantities for formation of the activated transition intermediate. This approach will be discussed in some detail below and in the Supporting Information. No attempts to satisfy the minimum requirements for model acceptance, such as obtaining absolute spectra and the macro kinetic constants from the data, were made.

In example 8, the RHM tested is similar to the one tested by Lozier et al. (1992) in example 3 and the same data were used. The determination of all kinetic constants, as well as was ΔH^* values, was based on the Eyring equation using data collected at different temperatures. This is the first paper in which a fully described RHM model was applied to experimental data to extract absolute spectra for the intermediates of the cycle. The authors presented their studies as a basis for acceptance of their tested model as the real model for the BR photocycle. For these reasons, plus the fact that Lozier kindly provided us with his data, we initiated the studies described in this paper to compare an "authenticated" RHM with our UPM model for the BR photocycle. It is important to note that, in their publication, van Stokkum and Lozier were able to extract essentially the same absolute intermediate spectra from their data using the entirely different kinetic model of example 6. If no more than one model can be true, this finding suggests that too many degrees of freedom may exist in the methods used.

In summary, to date, no proposed RHM has met minimum criteria for acceptance and there is no consensus in the field on which, if any, of the proposed RHM may be qualified as authentic. This uncertainty exists even though individual, but different, RHM have been substantiated by use of such powerful techniques as thermodynamics and electron and X-ray crystallographies.

Major Problems for Proving the RHM that Do Not Exist for the UPM. As pointed out by Nagle[38] and Dioumaev,[39] there is insufficient information to allow a unique determination of all the kinetic constants and amplitudes in a RHM from any single set of data obtained under one set of conditions. As one way to extract the required parameters, it was suggested to accumulate data under a variety of conditions such as varying temperatures. In this approach, it is assumed that the temperature dependence of the rate constants obeys an Arrenhius relationship in which the log of the constant is linear with the reciprocal of absolute temperature. As we show below and in the Supporting Information, the application of the Arrenhius equation to a connected array of state transitions may not be justified.

For UPM, where only macroconstants are involved, and they can be readily determined by fitting exponentials to the data, a solution is attainable for only a single set of data as demonstrated here and elsewhere.[3,4]

Problems with Applying either the Arrenhius or Eyring Equation to BR Photocycle Data to Obtain Kinetic Microconstants and Thermodynamic Parameters. In the Supporting Information, derivations of both equations are provided, and it is shown that the Arrenhius equation properly applies only to isolated equilibria for free reactants and products in a closed system. Many complications that exist for connected successive equilibria which occur in a BR photocycle for a system that is held in place by membrane lipids that control the structure, photocycle pathways, intermembrane mobility, and kinetics of the bR protein are discussed.

The Eyring equation was derived for a unidirectional forward conversion of free reactant to product in a closed system. Specifically, the equation applies to the reaction, $A \rightleftarrows A^* \Rightarrow B$. The equation does not deal with either the kinetics or thermodynamics of the reaction $A \rightleftarrows AB^* \rightleftarrows B$.

A considerably more complex equation is required to deal with a freely reversible series of reactions that are essential to any RHM. Furthermore, the Eyring equation does not support the use of a linear plot of $\ln(k)$ vs $1/T$ to obtain k values at different temperatures or the desired thermodynamic parameters. The relationship between $\ln(k)$ and T is

$$\ln(k) = \ln(k_B T/h) - (\Delta H^*/RT) + (\Delta S^*/R)$$

A plot of $\ln(k)$ vs $1/T$ will be influenced by the term $\ln(k_B T/h)$ at very low values of $1/T$ where temperatures are high. Near the y-intercept, where T approaches infinity, the curve will asymptotically rise and never meet the axis. Therefore, a valid value of $(\Delta S^*/R)$ cannot be obtained by extrapolation to the y-axis. The values obtained for k could also be in question. All of these uncertainties can be avoided by plotting $\ln(k/t)$ vs $1/T$ according to the equation

$$\ln(k/T) = \ln(k_B/h) - (\Delta H^*/RT) + (\Delta S^*/R)$$

This is an equation for a straight line with a valid y-intercept of $(\Delta S^*/R)$.

Evidence for Parallel Models. (1) In 1984, parallel models were proposed by Hanomoto et al.[40] on the finding that the kinetics of formation of two forms of M were different and that the ratio of amplitudes for the two was pH-dependent. The latter finding was explained by the fact that the rate constants of the fast M were pH-independent while that of the slow form was not. The findings were interpreted in terms of two separate pathways of L→M conversions arising from heterogeneity in ground-state BR. The heterogeneity was attributed a possible difference in environment for the protonated Schiff base, resulting from its proximity or removal from a local positive charge that could be a cation such as Ca^{2+} or Mg^{2+}. No specific photocycle model was presented.

(2) At the same time, either a parallel or branched model was proposed by Li et al.[41] to explain the opposite effects of pH on the amplitudes of the fast and slow forms of M and the opposite relationship to both forms of M. Other differences in function of the two forms of M were revealed by the opposite effects of temperature on their amplitudes and the observations that flash-induced proton release was correlated to the amplitude of M-slow, but not M-fast under conditions of change of pH or change of temperature. No specific photocycle model was proposed.

(3) Diller and Stockburger[42] (1986) used kinetic resonance Raman spectroscopy to demonstrate that there are two distinct forms of L intermediate with different decay times and which originate from two different forms of BR. They estimated that at 23 °C the population ratio of the two forms is 1.4:1. No specific photocycle model was proposed.

(4) Komrakov and Kaulen[43−45] (1993−1994) using optical spectroscopy reported that two separate forms of M are present in wild-type and mutant *Halobacteria*. From the kinetics of M formation and decay to BR at different pH values, it was concluded that two different forms of BR exist at neutral pH. No specific photocycle model was proposed.

(5) Eisfeld et al.[46] (1993) used a combination of resonance Raman and optical studies to examine the kinetics of the BR photocycles at different pH. They concluded that two different

forms of BR are present in nearly equal amounts. Each of the two excited parent ground states can decay back to the ground state through four different pathways, depending on pH. The following different sequence pathways were deduced from the data:

$$K \rightarrow L \rightarrow M_{slow} \rightarrow BR$$

$$K \rightarrow L \rightarrow M_{fast} \rightarrow N \rightarrow BR$$

$$K \rightarrow L \rightarrow M_{fast} \rightarrow O \rightarrow BR$$

$$K \rightarrow L \rightarrow M \rightarrow N \rightarrow BR$$

(6) Hendler et al.[47] (1994) found that the M_{fast} (M_f) decays on a path leading to the O intermediate whereas M_{slow} (M_s) decays directly to BR. This finding, plus the fact that the ratio of M_f to M_s is titrated by the intensity level of the laser flash, strongly supports a two-cycle model in which one cycle contains the $M_f \rightarrow O \rightarrow BR$ sequence and the other the $M_s \rightarrow BR$ sequence. The ability of light level to regulate the ratio of M_f/M_s in such a parallel model was demonstrated by Shrager et al.[48] (1995). No specific photocycle model was proposed.

(7) Drachev et al.[49] (1994) reported that the L intermediate consists of two species with different decay times, forming two different forms of M, consistent with parallel photocycles. No specific photocycle model was proposed.

(8) Luchian et al.[50] (1996) confirmed the findings (items 5 and 6 above) that M-fast decays directly to the O intermediate, whereas M-slow decays directly back to BR.

(9) Groma et al.[50] (1997) studied time-dependent anisotropy, which is a model-dependent phenomenon under partially saturating photoselection conditions. They examined various different models including both homogeneous and parallel types. The latter types were able to account for time-dependent changes in anisotropy without invoking chromophore reorientation. On the basis of fittings of the amplitudes of exponentials using real experimental data, they concluded that models involving parallel processes are more consistent with observations than are strictly homogeneous ones.

(10) Hendler et al. and Shrager et al.[3,4] (2001) introduced new methods for obtaining a completely defined UPM model from experimental data collected at neutral pH and ~20 °C. The procedures were based on a comprehensive search of all possible combinations of linear sequences of any length and any order of linking the fitted kinetic macroconstants needed to fully describe the kinetics of the system. The final solution was in the form of a system of ordinary differential equations which uniquely describe every transition in every cycle comprising the UPM. If the experimental data did not arise from unidirectional parallel cycles, no unique UPM solution would be found. No preconceived concepts of assumed sequences nor linkages of the transitions of the photocycle could influence the results, and the kinetics deduced in the analysis were not influenced by an input of presumably correct optical spectra for the intermediates. It was shown that a model consisting two parallel cycles was able to extract absolute spectra for all of the intermediates from the data that were consistent with spectra deduced from the raw data by many laboratories using nonmodel dependent methods. The UPM solution was

$$BR^* \rightleftharpoons L \rightleftharpoons M_f \rightleftharpoons N \rightleftharpoons O \rightleftharpoons BR$$

$$BR^* \rightleftharpoons L \rightleftharpoons M_s \rightleftharpoons BR$$

On the basis of the findings in the current paper, which demonstrate partial reversibility in parallel models under certain conditions, the abbreviation PRUPM will be used to describe such models.

Experimental Observations not Explained by RHM but Readily Explained by Parallel Models. (1) RHM models requires that (a) BR is homogeneous; (b) there is only one photocycle sequence and it is the same under all conditions such as pH and temperature; (c) all intermediate spectra are entirely the same under all conditions. Evidence questioning whether these requirements have been met has been published.[5] Heterogeneity of BR is strongly indicated in items 1, 5, 6, 9, and 10 listed just above. Further evidence has been obtained in retinal binding studies,[52] studies of changes in dielectric spectroscopy as a function of light intensity,[53] and the finding of two bands in the isoelectric focusing profile obtained from a highly purified purple membrane preparation.[54] Examples of different photocycles operating under different conditions are well documented by all ten citations in the list directly above.

(2) It has been shown that M_f decays through a route involving the O intermediate, whereas M_s decays directly to BR.[46,47,50]

(3) Three or four species of M are found in photocycles under certain conditions.[24,25,55]

(4) The three slowest M species can be converted to the fastest of the four species by addition of specific purple membrane lipids or by increasing the global hydropobicity of the membrane by addition of decane.[55]

(5) In native BR, the ratio of M_f to M_s occurring in the photocycle can be changed from nearly all the one form to nearly all of the other by a variety of different means such as changes in actinic light intensity,[47] electrochemical potential,[56] pH,[55] or the addition of decane.[55] This cannot be accounted for in a RHM unless it can be demonstrated that the kinetic microconstants linking the M intermediates to each other or to neighboring intermediates are affected by all of these disparate treatments. In only one case was an argument made for the ability of actinic light to alter microconstants to affect the M_f/M_s ratio,[57] but, as shown elsewhere,[5] the data presented do not support the interpretation.

Parallel cycles are readily consistent with every one of those observations. Reversible, homogeneous models are not. This serious problem for RHM models cannot be brushed aside by suggesting additional hypothetical and unproven modifications of an RHM, such as the idea that actinic light can alter the rates of specific kinetic micro constants. We are not aware of any observations that require RHM for their explanation nor any that exclude parallel models. In the Supporting Information, we use synthetic data sets constructed from the RHM and UPM models for pH 7 and 20 °C in comparison to experimental data obtained under these conditions to show that the data set constructed from the UPM model is more compatible with the experimental data. No single proposed RHM has been acceptable to all investigators seeking a solution for the true kinetic model, and none has been shown to meet minimum requirements for serious consideration as a true representation of the BR photocycle.

The establishment of a valid model for the BR photocycle is of great importance in determining how the structural change in each transition specifically contributes to the energy-transducing transport of a proton across the membrane. Based on the view of the RHM, as a single reversible photocycle in which M1 is directly converted to M_2, this step is considered to be central to the transport process.[37] In an intricate series of

experiments utilizing the D85N/D68N mutant, a detailed mechanism was deduced for proton transport which depends on the isomerization of retinal in the sequential transition of M_1 to M_2 such that the proton-accepting Schiff base which, in the former configuration (M_1), communicates with a channel on the extracellular side shifts its orientation to a channel on the cytoplasmic side.[58] Intense efforts involving X-ray crystallography[37,59] and cryoelectron microscopy[35] have been interpreted as producing structures for each intermediate of the photocycle in which the essential parts of the hypothesis have been confirmed with the certainty of atomic resolution. But if, in fact, the two forms of M are in separate photocycles, the logic underlying the above-described approach and the apparent confirmation of the hypothesis are undermined.

Acknowledgment. The author is grateful to Richard Lozier for providing the data of Xie et al. used in the analyses reported in this paper and to Richard Shrager for the mathematical treatment used to introduce back-reactions into the J-matrix.

Supporting Information Available: Detailed data for fittings, thermodynamics of the temperature coefficient for kinetic constants, and comparison of RHM and UPM using synthetic and experimental data. This material is available free of charge via the Internet at http://pubs.acs.org.

References and Notes

(1) Ohno, K.; Takeuchi, Y.; Yoshida, M. *Photochem. Photobiol.* **1981**, *33*, 573−578.
(2) Shrager, R. I.; Hendler, R. W.; Bose, S. *Eur. J. Biochem.* **1995**, *229*, 589−595.
(3) Hendler, R. W.; Shrager, R. I.; Bose, S. *J. Phys. Chem. B* **2001**, *105*, 3319−3328.
(4) Shrager, R. I.; Hendler, R. W. Supporting Information for Hendler et al. (ref 3) at http://pubs.acs.org.
(5) Shrager, R. I.; Hendler, R. W. *J. Phys. Chem. B* **2003**, *107*, 1708−1713.
(6) van Stokkum, I. H. M.; Lozier, R. *J. Phys. Chem. B* **2002**, *106*, 3477−3485.
(7) Xie, A. H.; Nagle, J. F.; Lozier, R. *Biophys. J.* **1987**, *51*, 627−635.
(8) Lozier, R. H.; Bogomolni, A.; Stoeckinius, W. *Biophys. J.* **1975**, *15*, 955−962.
(9) Becher, B.; Tokunaga, F.; Ebrey, T. G. *Biochemistry* **1978**, *17*, 2293−2300.
(10) Zimányi, L.; Keztheli, L.; Lanyi, J. K. *Biochemistry* **1989**, *28*, 5165−5172.
(11) Váró, G.; Duschl, A.; Lanyi, J. K. *Biochemistry* **1990**, *29*, 3798−3804.
(12) Gergely, C.; Zimányi, L.; Váró, G. *J. Phys. Chem. B* **1997**, *101*, 9390−9395.
(13) Borucki, B.; Otto, H.; Heyn, M. P. *J. Phys. Chem. B* **1999**, *103*, 6371−6383.
(14) Kulcsár, A.; Saltiel, J.; Zimányi, L. *J. Am. Chem. Soc.* **2001**, *123*, 3332−3340.
(15) Schara, A. Z.; Zorko, M.; Strancar, J. *Eur. Biophys. J. Biophys. Lett.* **2004**, *33*, 715−725.
(16) Nicolini, C.; Thiyagarajan, P.; Winter, R. *Phys. Chem. Chem. Phys.* **2004**, *6*, 5531−5534.
(17) Mukherjee, S.; Maxfield, F. R. *Ann. Rev. Cell Dev. Biol.* **2004**, *20*, 839−866.
(18) Sherfeld, B. K.; Kahya, N. Schwille, P. *Biophys. J.* **2004**, *87*, 1034−1043.
(19) Wisniewska, A.; Draus, J.; Subczynski, W. K.*Cell. Mol. Biol. Lett.* **2003**, *8*, 147−169,
(20) Maxfield, FR. *Curr. Opin. Cell Biol.* **2002**, *14*, 483−487.
(21) Ladhs, S. *Grasas Y Aceites* **2000**, *51*, 56−65.
(22) Zuvic-Butorac, M.; Muller, P.; Pomorski, T.; Libera, J.; Hermann, A.; Scgara, M. *Eur. J. Biophys. J. Biophys. Lett.***1999**, *28*, 302−311.
(23) Kobayashi, T.; Gu, F.; Gruenberg, J. *Semin. Cell Dev. Biol.* **1998**, *9*, 517−526.
(24) Joshi, M. K.; Bose, S.; Hendler, R. W. *Biochemistry* **1999**, *38*, 8786−8793.
(25) Mukhopadhyay, A. K.; Dracheva, S.; Bose, S.; Hendler, R. W. *Biochemistry* **1996**, *35*, 9245−9252.
(26) Hendler, R. W.; Barnett, S. M.; Dracheva, S.; Bose, S.; Levin, I. W. *Eur. J. Biochem.* **2003**, *270*, 1920−1925.
(27) Joshi, M. K.; Dracheva, S.; Mukhopadhyay, A. K.; Bose, S.; Hendler, R. W. *Biochemistry* **1998**, *37*, 14463−14470.
(28) Váró, G.; Lanyi, J. K. *Biochemistry* **1990**, *29*, 2241−2250.
(29) Váró G.; Lanyi, J. K. *Biochemistry* **1991**, *30*, 5008−5015.
(30) Váró G.; Lanyi, J. K. *Biochemistry* **1991**, *30*, 5016−5022.
(31) Lozier, R H.; Xie, A.; Hofrichter, J.; Clore, G. M. *Proc. Natl. Acad. Sci. U.S.A.* **1992**, *89*, 3610−3614.
(32) Zimányi, L.; Váró, G.; Chang, M.; Baofu, N.; Needleman, R.; Lanyi, J. K. *Biochemistry* **1992**, *31*, 8535−8543.
(33) Hessling, B.; Souvignier, G.; Gerwert, K. *Biophys. J.* **1993**, *65*, 1929−1941.
(34) Ludmann, K.; Gergely, C.; Váró, G. *Biophys. J.* **1998**, *75*, 3110−3119.
(35) Subramaniam, S.; Lindahl, M.; Bullough, P.; Faruqi, A. R.; Tittor, J.; Oesterhelt, D.; Brown, L.; Lanyi, J. K.; Henderson, R. *J. Mol. Biol.* **1999**, *287*, 145−161.
(36) Zimányi, L. *J. Phys. Chem. B* **2004**, *108*, 4199−4209.
(37) Lanyi, J. K.; Schobert, B. *Biochemistry* **2004**, *43*, 3−8.
(38) Nagle, J. F. *Biophys. J.* **1991**, *59*, 476−487.
(39) Dioumaev, A. K. *Biophys. Chem.* **1997**, *67*, 1−25.
(40) Hanamoto, J. H.; Dupuis, P.; El-Sayed, M. A. *Proc. Natl. Acad. Sci. U.S.A.* **1984**, *81*, 7083−7087.
(41) Li, Q.-Q.; Govindjee, R.; Ebrey, T. G. *Proc. Natl. Acad. Sci. U.S.A.* **1984**, *81*, 7079−7082.
(42) Diller, R.; Stockburger, M. *Biochemistry* **1988**, *27*, 7641−7651.
(43) Komrakov, A. Y.; Kaulen, A. D. *FEBS Lett.* **1993**, *313*, 248−250.
(44) Komrakov, A. Y.; Kaulen, A. D. *Biochem. Int.* **1993**, *30*, 461−469.
(45) Komrakov, A. Y.; Kaulen, A. D. *FEBS Lett.* **1994**, *340*, 207−210.
(46) Eisfeld, W.; Pusch, C.; Diller, R.; Lohrmann, R.; Stockburger, M. *Biochemistry* **1993**, *32*, 7196−7215.
(47) Hendler, R. W.; Dancshazy, Zs.; Bose, S.; Shrager, R. I.; Tokaji, Zs. *Biochemistry* **1994**, *33*, 4604−4610.
(48) Shrager, R. I.; Hendler, R. W.; Bose, S. *Eur. J. Biochem.* **1995**, *229*, 589−595.
(49) Drachev, L. A.; Kaulin, A. D.; Komrakov, A. Y. *Biochem. (Moscow)* **1994**, *59*, 95−102.
(50) Luchian, T.; Tokaji, Zs.; Dancshazy, Zs. *FEBS Lett.* **1995**, *229*, 55−59.
(51) Groma, G. I.; Bogomolni, R. A.; Stoeckenius, W. *Biochim. Biophys. Acta* **1997**, 69−85.
(52) Friedman, N.; Ottolenghi, M.; Sheves, M. *Biochemistry* **2003**, *421*, 1281−11288.
(53) Mostafa, H. I. A. *FEBS Lett.* **2004**, *571*, 134−140.
(54) Miercke, L. J. W.; Ross, P. E.; Stroud, R. M.; Dratz, E. A. *J. Biol. Chem.* **1989**, *264*, 7531−7535.
(55) Hendler, R. W.; Bose, S. *Eur. J. Biochem.* **2003**, *270*, 3518−3524.
(56) Hendler, R. W.; Drachev, L. A.; Bose, S.; Joshi, M. K. *Eur. J. Biochem.* **2000**, *267*, 5879−5890.
(57) Váró, G.; Needleman, R.; Lanyi, J. K. *Biophys. J.* **1996**, *70*, 461−467.
(58) Brown, L. S.; Dioumaev, A. K.; Needleman, R.; Lanyi, J. K. *Biochemistry* **1998**, *37*, 3982−3993.
(59) Kataoka, M.; Kamikubo, H. *Biochim. Biophys. Acta* **2000**, *1460*, 166−176.
(60) Felicia, M. H.; Glaeser, R. M. *Biochim. Biophys. Acta* **2000**, 1460, 106−118.
(61) Chizhov, I.; Chernavskii, D. S.; Engelhard, M.; Mueller, K.-H.; Zubov, B. V.; Hess, B. *Biophys. J.* **1996**, *71*, 2329−2345.
(62) Muller, K.-H.; Butt, H. J.; Bamberg, E.; Fendler, K.; Hess, B.; Siebert, F.; Engelhard, M. *Eur. Biophys. J.* **1991**, *19*, 241−251.